Theor Chem Acc (2006) 115: 190–195
DOI 10.1007/s00214-005-0052-6

REGULAR ARTICLE

Oleg V. Yazyev · Lothar Helm

Hyperfine interactions in aqueous solution of Cr^{3+}: an ab initio molecular dynamics study

Received: 19 May 2005 / Accepted: 28 July 2005 / Published online: 10 December 2005
© Springer-Verlag 2005

Abstract We performed an ab initio molecular dynamics simulation of the paramagnetic transition metal ion Cr^{3+} in aqueous solution. Isotropic hyperfine coupling constants between the electron spin of the chromium ion and nuclear spins of all water molecules have been determined for instantaneous snapshots extracted from the trajectory. The coupling constant of first sphere oxygen, $A_{iso}(^{17}O_I) = 1.9 \pm 0.3$ MHz, is independent on Cr–O_I distance but increases with the tilt angle for the water molecule approaching 180°. First sphere hydrogen spins have $A_{iso}(^{1}H_I) = 2.1 \pm 0.2$ MHz which decreases with increasing tilt angle and shows a Cr–H_I distance dependence. The hyperfine coupling constants for second sphere ^{17}O is negative and an order of magnitude smaller (-0.20 ± 0.02 MHz) compared to first sphere.

Keywords Ab initio molecular dynamics · Paramagnetic ion · Hyperfine coupling constants

1 Introduction

Historically, the computational methods for approximate solving of the Schrödinger equation have been developed rather separately in chemistry and physics. The reason for this division is fairly simple – chemists are mainly interested in molecules whereas physicists deal mainly with condensed matter. During the last decade, these fields mutually penetrated due to developments in the field of density functional theory and progress of computer technology.

O. V. Yazyev · L. Helm
Laboratoire de Chimie Inorganique et Bioinorganique,
Ecole Polytechnique Fédérale de Lausanne,
EPFL-BCH, CH-1015 Lausanne, Switzerland

L. Helm (✉)
Institut des Sciences et Ingénierie Chimiques,
Ecole Polytechnique Fédérale de Lausanne,
EPFL-BCH; CH-1015 Lausanne, Switzerland
E-mail: lothar.helm@epfl.ch
Tel: +41-21-6939876
Fax: +41-21-6939875

Nowadays, density functional theory using plane wave basis sets and pseudopotentials is de facto standard in condensed matter theory research. This approach offers two valuable advantages for chemists studying systems in solutions. First, the plane waves are naturally periodic functions and their use implies the imposition of periodic boundary conditions on a system. Therefore, one can simulate solutions using large enough simulation cells containing the solute and a sufficient number of solvent molecules. This technique is called *supercell approach*. Second, pseudopotential plane wave technique permits efficient implementations of ab initio molecular dynamics (AIMD). In contrast to classical molecular dynamics, AIMD is based on the electronic structure theory and does not use an empirical force field for the description of chemical bonds and non-bonding interactions. This simplifies its application to objects of coordination chemistry and allows simulations of chemical reactions involving bond breaking and formation as well as electron transfer. The evident disadvantage is the computational cost of AIMD simulations. Currently, the system size is limited to a few hundreds of atoms while a typical duration of simulation does not exceed a few picoseconds.

Nevertheless, a number of AIMD studies of ions in water solution are already available in the literature. Among these are simulations of H^+ [1,2], OH^- [3,4], Li^+ [5], K^+ [6], Be^{2+} [7], Mg^{2+} [8], Ca^{2+} [9], Al^{3+} [10], Cu^{2+} [11], Cl^- [12], Br^- [13], N_3^- [14] as well as the model redox reaction $Ag^{2+} + Cu^+ \rightarrow Ag^+ + Cu^{2+}$ between copper and silver ions [15].

In the present contribution, we extend the scope of ab initio simulated metal ions to the paramagnetic d^3 transition metal ion Cr^{3+}. Structure and dynamics of the first and second hydration shell of Cr^{3+} have been studied in the last ten years experimentally [16–22] and by classical molecular dynamics (MD) simulation [19,20,23,24]. Because of the first coordination shell being very inert, the bare Cr^{3+} ion can be replaced by its hydrate $[Cr(H_2O)_6]^{3+}$ in classical MD simulations. The group of Marcos developed interaction potentials for hydrated ion – water interactions using ab initio calculations [24–26]. The group of Rode used a

combined ab initio quantum mechanical/molecular mechanical (QM/MM) approach to study structure and dynamics of Cr^{3+} in aqueous solution [27]. The inert first coordination sphere, as well as strong hydrogen binding due to polarization of first sphere water molecules, leads to a well structured second coordination sphere. A residence time of water molecules in the second sphere of 128 ps at 298 K could be measured by ^{17}O NMR due to a significant hyperfine interaction between the electron spin of Cr^{3+} and the ^{17}O nuclear spin [19]. In our AIMD study we show that the second coordination sphere water molecules are subjected to a significant Fermi contact hyperfine field.

2 Methodology and theoretical foundations

The periodically repeated simulation box consisted of a Cr^{3+} ion and 54 water molecules. The dimension of the cubic box 11.513 Å× 11.513 Å× 11.513 Å were calculated on the basis of the experimental value for the absolute molar volume of Cr^{3+}, $V^{o}_{abs}(Cr^{3+}) = -52.9\,\mathrm{mol\,cm^{-3}}$ [28]. The first two coordination spheres of the chromium ion entirely fit into the box of this size (Fig. 1). The 3+ charge of the ion was neutralized by a uniform background charge.

AIMD calculations were performed using the CPMD3.9 code [29]. In our study we use a combined approach in which the calculation of the hyperfine parameters is performed at selected points of the MD simulation trajectory, so called "snapshots". The properties of interest are calculated at these "snapshots" after quenching the wavefunction of the system to the Born–Oppenheimer (BO) surface. Car-Parrinello AIMD simulations [30] do not follow BO surface precisely and the spin density distribution in the system tends to be more delocalized which may significantly decrease the accuracy of calculated hyperfine coupling constants. Also, such a methodology permits us to use higher plane-wave (PW) cutoffs and specially tailored pseudopotentials in our property calculations. In both cases we use the Becke exchange density functional [31] in combination with the Lee–Yang–Parr correlation density functional [32] (BLYP). The calculations were performed in unrestricted manner in order to take into account spin-polarization effects. The MD simulation was carried out for 2.5 ps after an initial equilibration of 1 ps. Limitations due to short simulation time were compensated by the altered temperature which was kept around 350 K. Hyperfine coupling constants are in general not temperature dependent. The fictitious electron mass was set to 600 a.u. The time step used was equal to 5 a.u. (0.121 fs). Hydrogen nuclei were treated classically and had a mass of the deuterium isotope. For the MD simulation we used Vanderbilt ultrasoft pseudopotentials [33] with a [Ne] core configuration for the Cr^{3+}. In addition, a nonlinear core correction was used on the paramagnetic ion. The plane-wave kinetic energy cutoff for valence electron wavefunctions was set to 30 Ry.

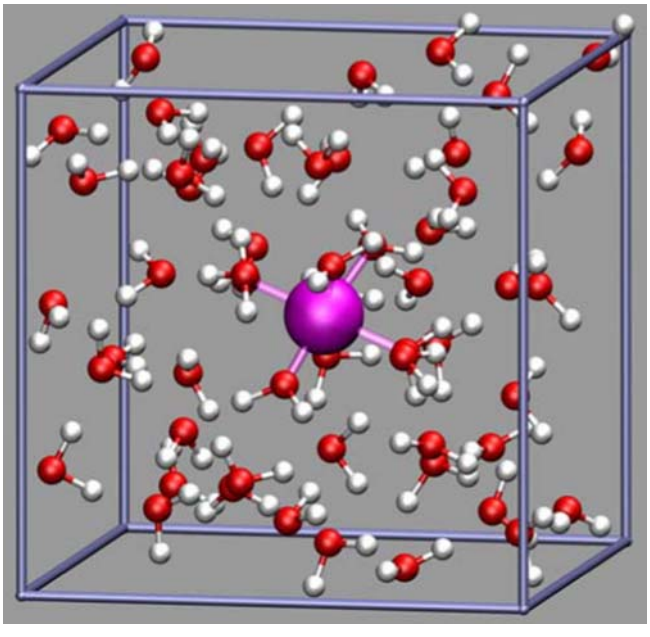

Fig. 1 A typical configuration of the ab initio molecular dynamics simulation of Cr^{3+} with 54 water molecules in a cubic box at 350 K

For the calculation of isotropic hyperfine coupling constants, A_{iso}, five snapshots were used, extracted from the MD trajectory in 0.5 ps intervals. Thus, 30 $A_{iso}(^{17}O_I)$, 60 $A_{iso}(^{1}H_I)$ for first sphere water and approximately 60 $A_{iso}(^{17}O_{II})$ for second sphere water are available for statistical analysis. The total amount of 270 of $A_{iso}(^{17}O)$ and 540 values of $A_{iso}(^{1}H)$ was calculated for the whole system. This amount of data is sufficient for reliable statistical averaging. The interval of time sampled is enough to provide the averaging over the molecular vibrations in the system. Since only octahedral coordination of the Cr^{3+} ion in aqueous solution is expected, we suggest that the time interval of 2.5 ps is enough to get accurate mean values. The statistical errors of the calculated hyperfine couplings are standard deviations of the mean. The valence wavefunctions in the property calculations were expanded in the plane wave basis set to a cutoff of 80 Ry. In these calculations we used norm-conserving Troullier–Martins pseudopotentials [34] with a $[Ne]3s^2 3p^6$ core configuration for chromium. The wavefunctions were converged with the preconditioned conjugate gradient method using a maximum value of 10^{-6} for the largest element of the gradient of the wavefunction. The nonlinear core correction [35] was used on both chromium and oxygen.

The isotropic (Fermi contact) hyperfine coupling constant on nucleus N is given by

$$A_{iso}(N) = \frac{4\pi}{3S}\beta_e\beta_N g_e g_N \rho^{\alpha-\beta}(\mathbf{R}_N),$$

where β_e and β_N are the Bohr and nuclear magnetons, respectively, g_e and g_N are free-electron and nuclear g-values, and S is the total electronic spin of the atom, ion or molecule. The electron spin density $\rho^{\alpha-\beta}(\mathbf{R}_N)$ at the point of nucleus N is the difference between the majority spin (α) and the minority spin (β) densities, $\rho^{\alpha-\beta}(\mathbf{R}_N) = \rho^{\alpha}(\mathbf{R}_N) - \rho^{\beta}(\mathbf{R}_N)$. The ^{1}H water isotropic hyperfine coupling constants and valence contribution to ^{17}O water hyperfine coupling con-

stants were calculated from pseudopotential spin density using the method of Van de Walle and Blöchl [36]. The 1 s core spin-polarization contribution to ^{17}O hyperfine coupling constants was calculated using the frozen valence spin-density atomic calculations according to Yazyev et al. [37].

3 Results and discussion

3.1 Coordination number and radial distribution functions

The Cr–O and Cr–H radial distribution functions (RDF) of the AIMD simulation are given in Fig. 2. The octahedral coordination sphere was stable and no first coordination sphere water exchange events were observed during the simulation. The average Cr–O_I distance in the first coordination sphere is 2.033 Å, and the Cr–H_I distance is 2.696 Å. The Cr–O_I distance compares well with existing experimental values of 2.03 ± 0.02 Å (large angle X-ray diffraction [38]), 1.97–1.99 Å (X-ray diffraction [39–41]), 1.98 Å (neutron diffraction [42]), 1.97–2.01 Å (extended X-ray absorption fine structure [21,22,38]) and other theoretical studies [19, 25,27,43,44] (see also Table 1 in ref. [19] and Table 1 in ref. [27]).

The Cr–O RDF shows a well pronounced second coordination sphere of Cr^{3+} in aqueous solution. The limit of the second coordination sphere, determined on the basis of the second minimum of Cr–O RDF, is 4.75 Å. The second sphere coordination number is 12.6 and the average Cr–O_{II} distance is 4.17 Å. The available experimental data give values of 12–14 for the second sphere coordination number and 3.95–4.25 Å for the Cr–O_{II} distance [21,25,38–40,42,43]. The combined QM/MM study [27] led to a slightly longer Cr–O_{II} distance of 4.36 Å and connected that to a higher second sphere coordination number of 15.4.

The distribution of oxygen atoms of water molecules outside the first coordination sphere around first shell oxygen atoms, O_I, is shown in Fig. 3. From the maximum of the first peak a $O_I - O_{II}$ distance of 2.67 Å is obtained. This value is markedly longer as the 2.41 Å found in a classic MD simulation [19]. However, the agreement with results from classical MD using more sophisticated interaction potentials (2.58–2.60 Å [20,23]) as well as experimental data (2.60–2.63 Å [38]) is very satisfactory.

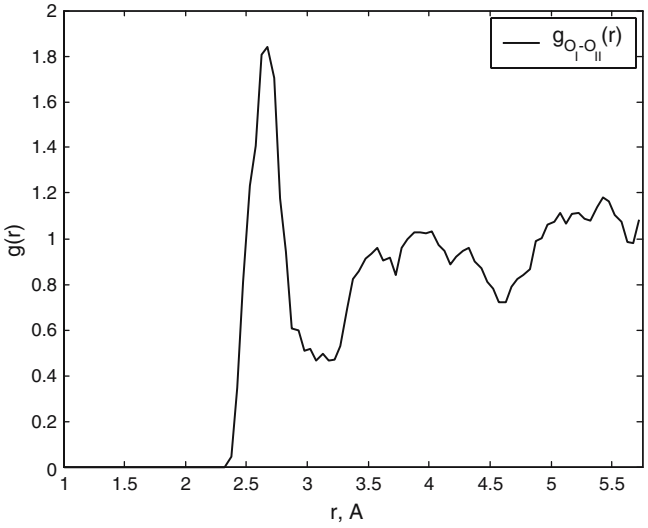

Fig. 3 The RDF of water oxygen outside the first coordination sphere around first shell oxygen atoms O_I

3.2 Hyperfine coupling constants

Figures 4 and 5 show the dependence of $A_{iso}(^{17}O)$ and $A_{iso}(^{1}H)$ on the Cr–O and Cr–H distances, respectively. The mean isotropic scalar coupling constant of $\langle A_{iso}(^{17}O_I)\rangle = 1.9 \pm 0.3$ MHz for first coordination sphere water molecules corresponds to a negative average value of spin-density on the $^{17}O_I$

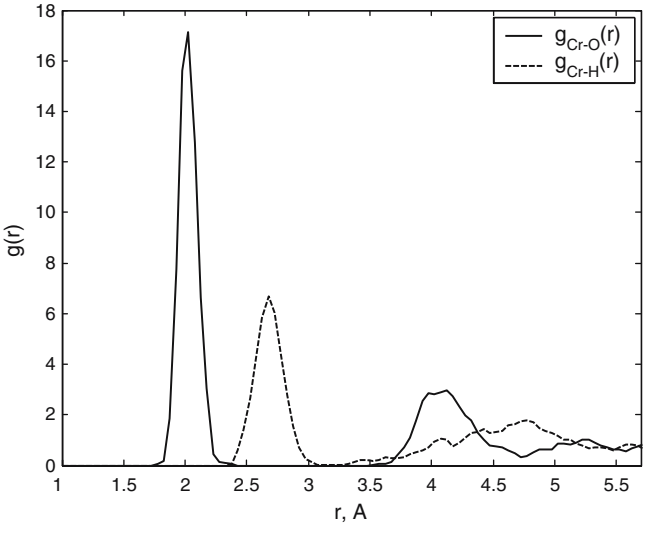

Fig. 2 The Cr–O and Cr–H radial distribution functions (RDF)

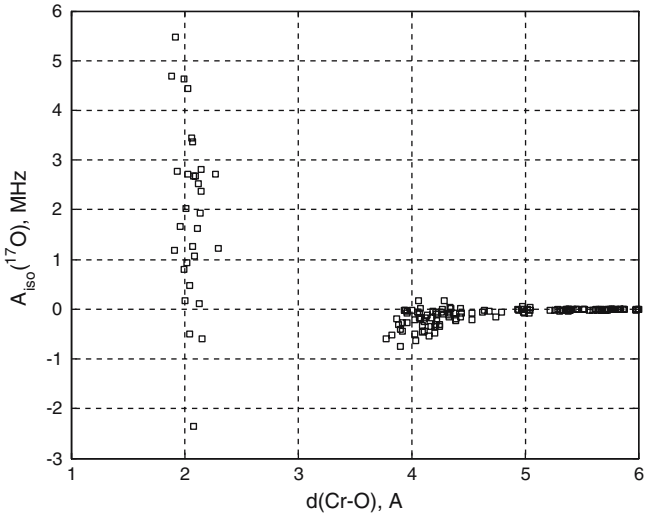

Fig. 4 Isotropic scalar coupling constant, $A_{iso}(^{17}O)$, as a function of the Cr–O distance from five snapshots

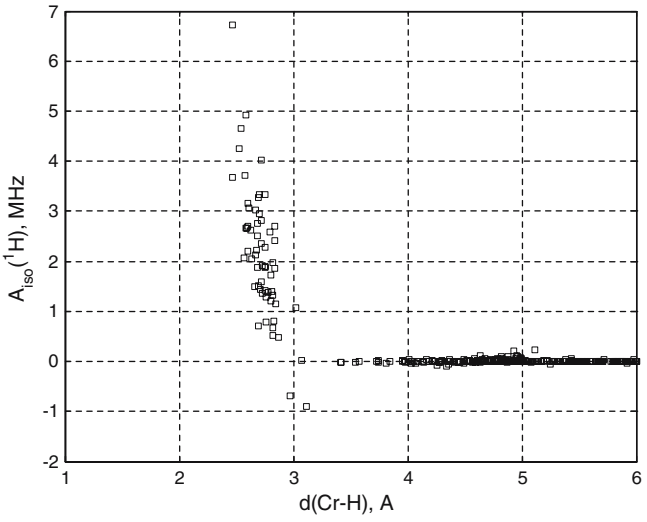

Fig. 5 Isotropic scalar coupling constant, $A_{iso}(^1H)$, as a function of the Cr–H distance

nuclei, due to a negative gyromagnetic ratio for ^{17}O. This suggests a strong spin-polarization mechanism of the distribution of unpaired electron density in the first coordination sphere (Fig. 6, top). However, the positive value observed for first shell water protons, $\langle A_{iso}(^1H_I)\rangle = 2.1 \pm 0.2$ MHz, corresponds to a positive value of spin density at the positions of ^1H_I nuclei. The $A_{iso}(^1H_I)$ values also show a clear dependence on the Cr–H_I distance (Fig. 5). A possible explanation is that the spin-delocalization depends on the tilt angle θ for first sphere water molecules (Figs. 7, Fig. 8) which is commonly defined as the deviation from a radial alignment of the water dipoles. The $A_{iso}(^{17}O_I)$ increases when θ approaches radial alignment of water dipoles, but at the same time $A_{iso}(^{17}O_I)$ shows no visible dependence on the Cr–O_I distance. However, $A_{iso}(^1H_I)$ decreases with θ approaching 180°, and shows therefore a dependence on the Cr–H_I distance with a negative slope. The experimentally measured value for $A_{iso}(^1H_I)$ is 2.1 MHz [44,45], in prefect agreement with our calculations. No experimental $A_{iso}(^{17}O_I)$ value is available due to very slow exchange of first shell water molecules on Cr^{3+}.

Our calculations show also considerable spin-delocalization on the second coordination sphere water molecules (Fig. 6, bottom) leading to negative $A_{iso}(^{17}O_{II})$ values for r(Cr–O) values between 3.7 and 4.8 Å (Fig. 4). It is worth noting that while the spin polarization over second coordination sphere bears mainly negative character (see Fig. 6, bottom) the positive spin density at the positions of $^{17}O_{II}$ nuclei prevails. The average value for second coordination sphere water is $\langle A_{iso}(^{17}O_{II})\rangle = -0.20 \pm 0.02$ MHz which is an order of magnitude smaller than $\langle A_{iso}(^{17}O_I)\rangle$. Our calculated value is in agreement with the experimental values of −0.215 MHz and of −0.24 MHz [19,46] (recalculated for a second sphere coordination number of 12).[1] An interesting feature is the change in sign of $A_{iso}(^{17}O)$ from positive to negative between first and second coordination sphere. Such a behavior has been observed experimentally on $[Ti(H_2O)_6]^{3+}$ [47]. The outer sphere chemical shift of the ^{17}O NMR resonance is about 5% of the first sphere shift with a negative sign. Golding and Stubbs calculated as early as in 1979 isoshielding maps for a d^1 transition metal ion in a strong crystal field [48]. From their calculations, water oxygen sitting close to the triangular faces of the octahedron formed by the

[1] Note the incorrect sign of $A_{iso}(^{17}O)$ in the cited publications.

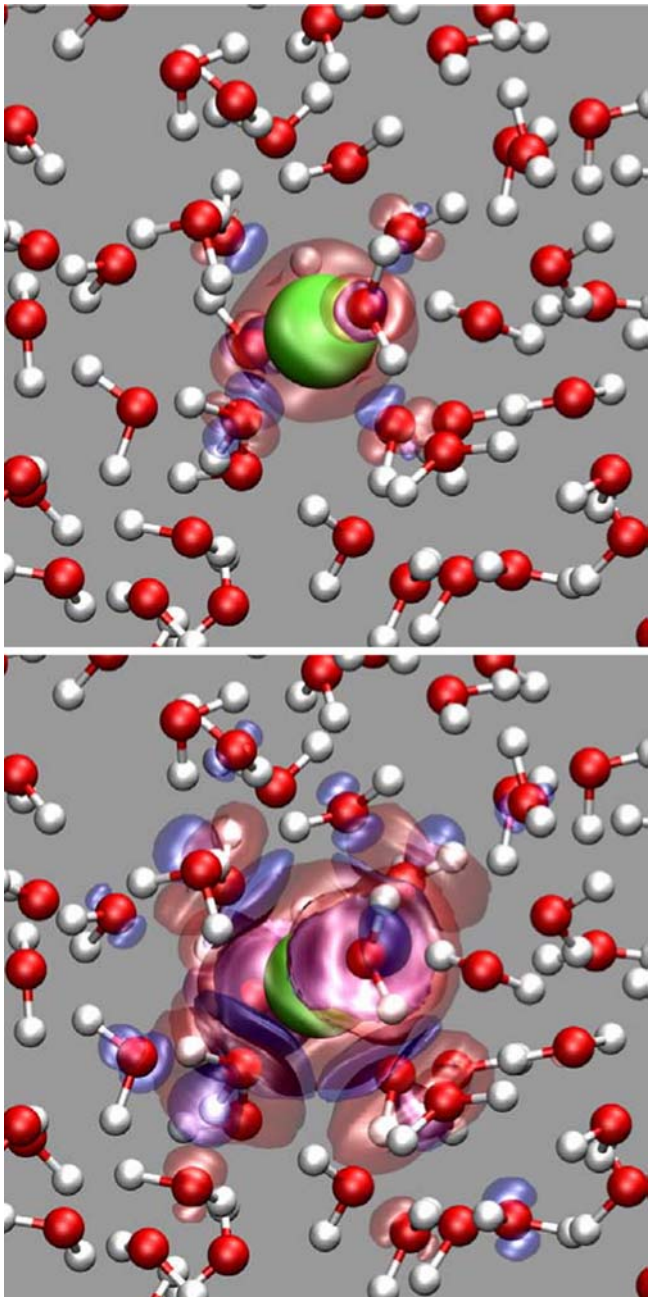

Fig. 6 Isosurface plots of the spin-density distribution around the paramagnetic Cr^{3+} for an isovalue of 0.002 a.u.$^{-3}$ (*top*) and 0.0001 a.u.$^{-3}$ (*bottom*). The positive (excess spin) spin-density is shown in red and the negative spin density is shown in blue. The spin-polarization of second coordination sphere water molecules can be observed (*bottom*)

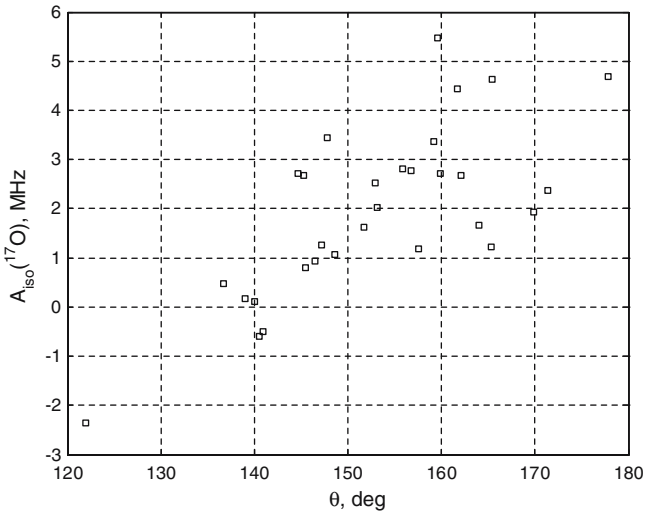

Fig. 7 Isotropic scalar coupling constant, $A_{\mathrm{iso}}(^{17}\mathrm{O})$ as function of the tilt angle θ

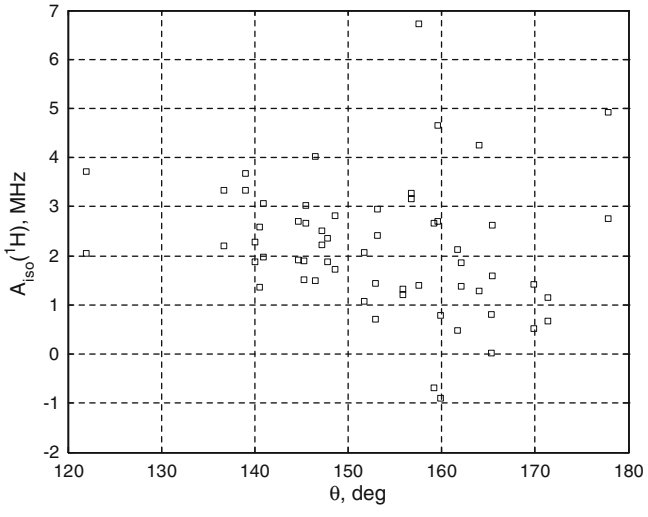

Fig. 8 Isotropic scalar coupling constant, $A_{\mathrm{iso}}(^{1}\mathrm{H})$, as a function of the tilt angle θ

coordinated water molecules have opposite chemical shifts in respect to those on the vertices of the octahedron.

Hyperfine coupling to second sphere water molecules is also observed on polyaminocarboxylate complexes of gadolinium(III), used as contrast agents in magnetic resonance imaging in medicine [49]. On these complexes, water exchange of the first sphere water molecule is relatively slow and an outer sphere term has to be used to fit the chemical shift data. This outer sphere term is in general 1/10 of the first sphere term which nicely corroborates with our findings [50]. In the case of the Gd^{3+} aqua ion $[Gd(H_2O)_8]^{3+}$ such a term could not be quantified because water exchange is very fast [51].

4 Conclusions

We performed an AIMD simulation of the paramagnetic transition metal ion Cr^{3+} in aqueous solution. The simulation reproduces experimental Cr^{3+} – oxygen distances of the first coordination sphere of the ion and proves the existence of well defined second coordination sphere consisting of about 12 water molecules. Isotropic hyperfine coupling constants are calculated from snapshots of the AIMD simulation. First sphere $^{1}H_{I}$ and second sphere $^{17}O_{II}$ hyperfine coupling constants are in excellent agreement with experimental results. The value of the second coordination sphere water molecule ^{17} O isotropic hyperfine coupling shows significant unpaired electron delocalization even in the second coordination sphere of Cr^{3+}.

Acknowledgements We acknowledge Jürg Hutter for providing us with the starting configuration of a metal hexaaquaion in water box. The calculations were carried out at the Swiss Center for Scientific Computing (Manno). This research was supported by the Swiss National Science Foundation and the Office for Education and Science, and was carried out in the EC COST Action D18.

References

1. Marx D, Tuckerman ME, Hutter J, Parrinello M (1999) Nature 397:601–604
2. Geissler PL, Dellago C, Chandler D, Hutter J, Parrinello M (2000) Chem Phys Lett 321:255
3. Tuckerman ME, Marx D, Parrinello M (2002) Nature 417:925
4. Geissler OL, Dellago C, Chandler D, Hutter J, Parrinello M (2001) Science 291:2121
5. Lyubartsev AP, Laasonen K, Laaksonen A (2001) J Chem Phys 114:3120
6. Ramaniah LM, Bernasconi M, Parrinello M (1999) J Chem Phys 111:1587
7. Marx D, Sprik M, Parrinello M (1997) Chem Phys Lett 273:360
8. Lightstone FC, Schwegler E, Hood RQ, Gygi F, Galli G (2001) Chem Phys Lett 343:549
9. Bako I, Hutter J, Palinkas G (2002) J Chem Phys 117:9838
10. Lubin MI, Bylaska EJ, Weare JH (2000) Chem Phys Lett 322:447
11. Pasquarello A, Petri I, Salmon PS, Parisel O, Car R, Tóth E, Powell DH, Fischer HE, Helm L, Merbach AE (2001) Science 291:856
12. Tobias DJ, Jungwirth P, Parrinello M (2001) J Chem Phys 114:7036
13. Raugei S, Klein ML (2002) J Chem Phys 116:196
14. Yarne DA, Tuckerman ME, Klein ML (2000) Chem Phys 258:163
15. Blumberger J, Bernasconi L, Tavernelli I, Vuilleumier R, Sprik M (2004) J Am Chem Soc 126:3928
16. Munoz-Paez A, Sanchez Marcos E (1992) J Am Chem Soc 114:6931
17. Munoz-Paez A, Pappalardo RR, Sanchez Marcos E (1995) J Am Chem Soc 117:11710
18. Diáz-Moreno S, Munoz-Paez A, Martinez JM, Pappalardo RR, Sanchez Marcos E (1996) J Am Chem Soc 118:12654
19. Bleuzen A, Foglia F, Furet E, Helm L, Merbach AE, Weber J (1996) J Am Chem Soc 118:12777
20. Sakane H, Munoz-Paez A, Díaz-Moreno S, Martinez JM, Pappalardo RR, Sanchez Marcos E (1998) J Am Chem Soc 120:10397
21. Merkling P, Munoz-Paez A, Martinez JM, Pappalardo RR, Sanchez Marcos E (2001) Phys Rev B 64:12201
22. Merkling P, Munoz-Paez A, Sanchez Marcos E (2002) J Am Chem Soc 124:10911
23. Martinez JM, Pappalardo RR, Sanchez Marcos E, Refson K, Díaz-Moreno S, Munoz-Paez A (1998) J Phys Chem B 102:3272

24. Martinez JM, Pappalardo RR, Sanchez Marcos E (1999) J Am Chem Soc 121:3175
25. Martinez JM, Hernandez-Cobos J, Pappalardo RR, Ortega-Blake I, Sanchez Marcos E (2000) J Chem Phys 112:2339
26. Pappalardo RR, Sanchez Marcos E (1993) J Phys Chem 97: 4500
27. Kritayakornupong C, Plankensteiner K, Rode BM (2004) J Comp Chem 25:1576
28. Swaddle TW, Mak MKS (1983) Can J Chem 61:473
29. Copyright IBM Corp 1990–2004, Copyright MPI für Festkörperforschung Stuttgart (1997–2001)
30. Car R, Parrinello M (1985) Phys Rev Lett 55:2471
31. Becke AD (1988) Phys Rev A 38:3098
32. Lee C, Yang W, Parr RG (1988) Phys Rev B 37:785
33. Vanderbilt D (1990) Phys Rev B 41:7892
34. Troullier N, Martins J (1991) Phys Rev B 43:1993
35. Louie SG, Froyen S, Cohen ML (1982) Phys Rev B 26:1738
36. Van de Walle CG, Blöchl PE (1993) Phys Rev B 47:4244
37. Yazyev OV, Tavernelli I, Helm L, Röthlisberger U (2005) Phys Rev B 71:115110
38. Read MC, Sandström M (1992) Acta Chem Scand 46:1177
39. Caminiti R, Licheri G, Piccagula G, Pinna G (1978) J Chem Phys 69:1
40. Bol W, Welzen T (1977) Chem Phys Lett 49:189
41. Magini M (1980) J Chem Phys 73:2499
42. Broadbent RD, Neilson GW, Sanström M (1992) J Phys Condens Matter 4:639
43. Pappalardo RR, Martínez JM, Sanchez Marcos E (1996) J Phys Chem 100:11748
44. Melton BF, Pollak VL (1969) J Phys Chem 73:3669
45. Bertini I, Fragai M, Luchinat C, Parigi G (2001) Inorg Chem 40:4030
46. Earl WL (1975) Thesis, University of California
47. Hugi AD, Helm L, Merbach AE (1987) Inorg Chem 26:1763
48. Golding R, Stubbs L (1979) J Magn Reson 33:627
49. Tóth É, Helm L, Merbach AE (2001) In: The chemistry of contrast agents in medical magnetic resonance imaging. Wiley, Chichester, 350 p 45
50. Powell DH, Ni Dhubhghaill OM, Pubanz D, Helm L, Lebedev YS, Schlaepfer W, Merbach AE (1996) J Am Chem Soc 118:9333
51. Micskei K, Powell DH, Helm L, Brücher E, Merbach AE (1993) Magn Reson Chem 31:1011